

# Contextual Memory-Enhanced Source Coding for Low-SNR Communications

Ziqiong Wang and Rongpeng Li

**Abstract**—While Separate Source-Channel Coding (SSCC) retains the practical benefits of modular system design, its effectiveness in noisy text transmission is fundamentally constrained by the fragility of autoregressive source decoding. In low-SNR regimes, even a small number of residual bit errors after channel decoding may derail the subsequent lossless reconstruction process, especially when Arithmetic Coding (AC) relies on Large Language Model (LLM)-based probability estimation. Existing remedies either strengthen channel decoding based solely on channel observations or introduce contextual information only at the receiver for post-hoc correction, yet neither fully addresses the fragility of source probability modeling under residual channel errors. To this end, this paper proposes a Memory-Augmented Source Coding (MASC) scheme for robust SSCC-based transmission. Rather than treating context as external side information, MASC internalizes contextual patterns into a source model shared by both the transmitter-side source encoder and the receiver-side source decoder. Specifically, MASC employs a shared Parameterized Contextual Memory (PCM) to encode multi-order  $n$ -gram patterns, and further introduces a Mixture-of-Memory-Experts Router (MMER) to perform sparse, hidden-state-dependent routing over memory experts during autoregressive source modeling. By adaptively activating only the most relevant memories at each coding step, MASC refines source probability estimation, shortens average codelength, and mitigates the sensitivity of source decoding to residual channel errors. Extensive experiments over Rayleigh fading and AWGN channels demonstrate the effectiveness of the proposed scheme compared with state-of-the-art methods.

**Index Terms**—Separate Source-Channel Coding (SSCC), arithmetic coding, memory-augmented source modeling, sparse expert routing.

## I. INTRODUCTION

Semantic Communications (SemCom) have emerged as a transformative paradigm [1]–[3], by leveraging Joint Source-Channel Coding (JSCC) to combat channel non-stationarity [4]–[6]. Nevertheless, Separate Source-Channel Coding (SSCC) remains a cornerstone of practical communication systems due to its inherent modularity and seamless integration with existing industrial standards [7]–[9]. However, the primary obstacle to deploying neural SSCC in practical noisy environments is the “cliff effect”. Due to the sequential dependency of compressed bitstreams, even a small number of residual bit errors after channel decoding may catastrophically break subsequent source decoding. Conventional remedies primarily focus on the channel-coding side,

employing advanced decoders like the Error Correction Code Transformer (ECCT) [10] to mitigate noise through code-aware inductive biases. Nevertheless, such decoders remain fundamentally constrained by channel observations alone [11], without introducing explicit external information.

To bridge this gap, recent advances have leveraged contextual information [12]–[14] at the receiver as a backward-compatible means to enhance robustness. Representative techniques include candidate maintenance [15], backtracking [16], and stochastic sampling [17]. Along this direction, our recent study further proposed a receiver-side in-context decoding framework that couples ECCT-assisted channel decoding with Large Language Model (LLM)-based source decoding, where contextual information and channel-decoding reliability are jointly used to enhance performance [18]. However, its effectiveness still hinges on sufficiently reliable contextual information at the receiver, which may be difficult to guarantee in practice. More fundamentally, such context is introduced merely as external side information at the receiver, rather than internalized into a shared memory that directly supports source probability modeling at both the transmitter and the receiver.

In this paper, we propose a Memory-Augmented Source Coding (MASC) framework, which leverages a shared Parameterized Contextual Memory (PCM) to alleviate the cliff effect. Departing from conventional Engram-based architectures [19] that rely on static look-up tables, MASC introduces a Mixture-of-Memory-Experts Router (MMER) within the PCM architecture. Rather than performing an exhaustive search across all stored patterns, the MMER leverages the latent hidden states of the previous Transformer block to adaptively and sparsely activate a subset of memory experts relevant to the current coding step. This mechanism enables MASC to retrieve multi-order  $n$ -gram representations that encompass a wide spectrum of semantic granularity. By injecting the retrieved memories into the subsequent Transformer block, MASC transforms transient context into persistent and trainable representations. Consequently, the shared memory provides a stable semantic foundation for probability modeling that effectively shortens the average codelength and thereby mitigates the fragility of the transmission against channel noise. We conduct extensive evaluations and demonstrate the effectiveness of MASC over conventional SSCC baselines, represented by Huffman-SSCC and ECCT-aided scheme [7], representative JSCC schemes, including DeepSC [20], Universal Transformer (UT) [21], and UT with quantization [22], as well as receiver-side in-context decoding methods such as ICD [18].

The remainder of the paper is organized as follows. Sec.

This is a preliminary version. Additional experiments and analysis will be included in future revisions.

Z. Wang and R. Li are with the College of Information Science and Electronic Engineering, Zhejiang University (email: {wangziqiong, lirongpeng}@zju.edu.cn).

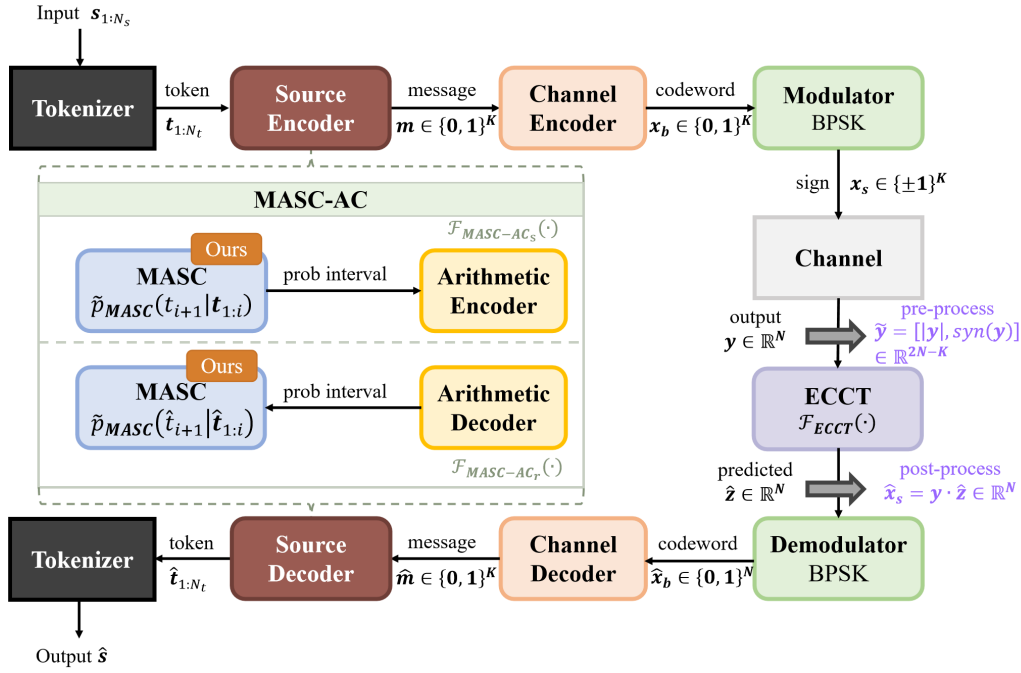


Fig. 1. Framework of the Proposed MASC-Based SSCC System.

II briefly introduces the system model and formulates the problem. Sec. III presents the overview of our proposed MASC scheme. In Sec. IV, we elaborate on the experimental results and discussions. Finally, Sec. V concludes the paper.

## II. PRELIMINARIES AND SYSTEM MODEL

### A. System Model

We consider an SSCC-based text transmission framework as illustrated in Fig. 1. For the  $N_s$ -length input text sequence  $\mathbf{s}_{1:N_s}$ , LLM-based Arithmetic Coding (AC) [23] is employed for source coding [7]. Specifically, the source sequence is first tokenized into  $\mathbf{t}_{1:N_t}$  with  $t_i \in \mathcal{D}$ , and a pre-trained LLM provides the conditional probabilities  $\tilde{p}_{\text{LLM}}(t_{i+1} | \mathbf{t}_{1:i})$  that drive the AC procedure. The overall source encoding process can be abstracted as

$$\mathbf{m} = \mathcal{F}_{\text{LLM-AC}_s}(\mathbf{s}_{1:N_s}) \in \{0, 1\}^K, \quad (1)$$

where  $\mathcal{F}_{\text{LLM-AC}_s}(\cdot)$  denotes a LLM-compatible source encoder that maps text into a length- $K$  bitstream through tokenization and probability-driven AC. The same pipeline can also be applied to other discrete sources (e.g., images) after appropriate lossless formatting or compression.

The message  $\mathbf{m}$  is then protected by an  $(N, K)$  Low-Density Parity-Check (LDPC) channel code as

$$\mathbf{x}_b = \mathbf{m}\mathbf{G} \pmod{2} \in \{0, 1\}^N, \quad (2)$$

where  $\mathbf{G} \in \{0, 1\}^{K \times N}$  is the generator matrix. The corresponding parity-check matrix  $\mathbf{H} \in \{0, 1\}^{(N-K) \times N}$  satisfies

$$\mathbf{G}\mathbf{H}^\top = \mathbf{0}. \quad (3)$$

Notably, other error correction codes such as Polar codes [24] can be applied as well [10]. The binary codeword  $\mathbf{x}_b$  is modulated via Binary Phase-Shift Keying (BPSK) as

$$\mathbf{x}_s = \mathbf{1} - 2\mathbf{x}_b \in \{\pm 1\}^N, \quad (4)$$

and transmitted over the channel according to

$$\mathbf{y} = h\mathbf{x}_s + \mathbf{z}, \quad \mathbf{z} \sim \mathcal{N}(\mathbf{0}, \sigma_n^2 \mathbf{I}), \quad (5)$$

where  $h$  denotes the channel coefficient and  $\mathbf{z}$  is the additive Gaussian noise.

At the receiver, we adopt the Error Correction Code Transformer (ECCT)<sup>1</sup> [10] to mitigate channel impairments. By exploiting the channel observations  $\mathbf{y}$  alongside the algebraic constraints of  $\mathbf{H}$ , ECCT produces an estimated disturbance  $\hat{\mathbf{z}}$  as well as a recovered BPSK-coded sequence  $\hat{\mathbf{x}}_s$ . The binary codeword estimate is then obtained via hard-decision demodulation as

$$\hat{\mathbf{x}}_b = \text{sign\_to\_bin}(\hat{\mathbf{x}}_s) \in \{0, 1\}^N, \quad (6)$$

where  $\text{sign\_to\_bin}(\hat{\mathbf{x}}_s) \triangleq \frac{1}{2}(\mathbf{1} - \text{sign}(\hat{\mathbf{x}}_s)) \in \{0, 1\}^N$ . We consider a systematic channel encoder, such that the information bits occupy the first  $K$  positions of the codeword. In this case, recovering the information bitstream reduces to extracting the first  $K$  bits as

$$\hat{\mathbf{m}} = \hat{\mathbf{x}}_{b,1:K} \in \{0, 1\}^K, \quad (7)$$

Given the channel decoding result  $\hat{\mathbf{m}}$ , an LLM-based source decoder  $\mathcal{F}_{\text{LLM-AC}_r}(\cdot)$  can eventually produce a reconstructed sequence  $\hat{\mathbf{s}}$  as follows

$$\hat{\mathbf{s}} = \mathcal{F}_{\text{LLM-AC}_r}(\hat{\mathbf{m}}). \quad (8)$$

<sup>1</sup>Complete architectural and training details of ECCT can be found in [10].

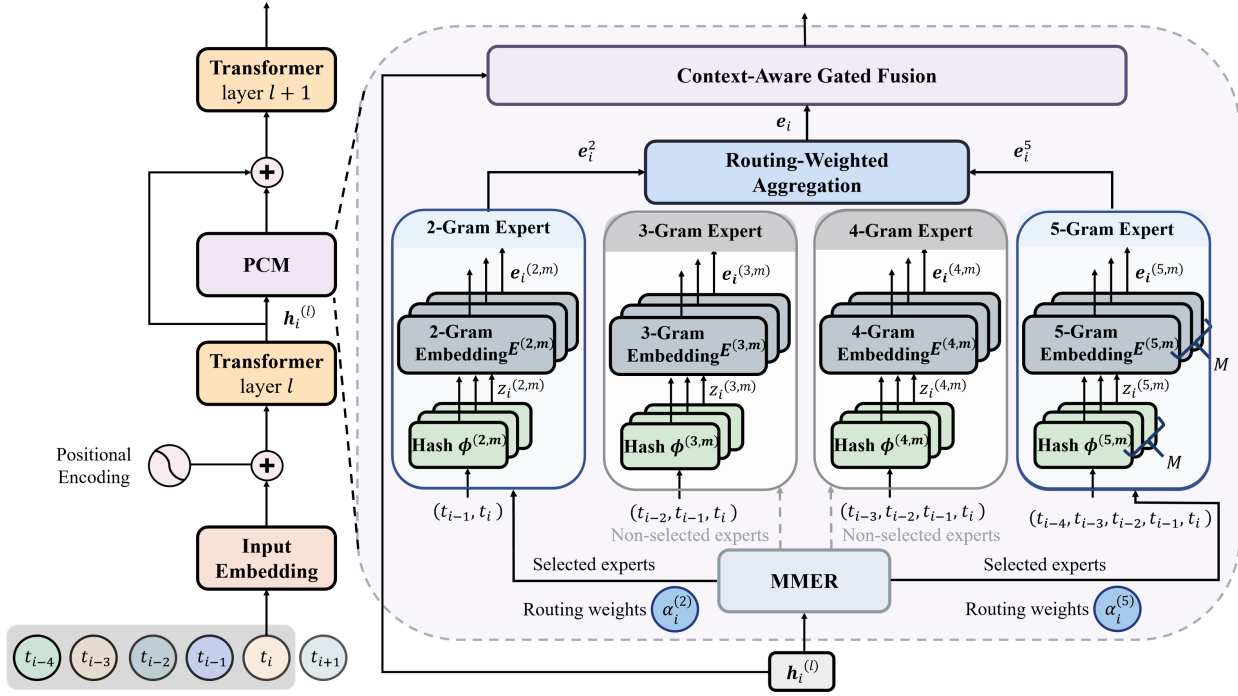


Fig. 2. The MASC Architecture.

## B. Problem Formulation

Conventional SSCC systems often suffer from a *cliff effect* in low-SNR scenarios. As illustrated by the purple line in Fig. 3 and Fig. 4, once the channel quality drops below a specific SNR threshold, a small number of residual bit errors may catastrophically disrupt the subsequent LLM-based arithmetic decoding process. The primary reason lies in the fact that an incorrect early bit can shift the LLM-based decoder to a wrong sub-interval for arithmetic decoding, which then perturbs subsequent token boundary decisions and triggers error propagation across many tokens. Consequently, the robustness of SSCC-based transmission depends not only on the reliability of channel decoding, but also on the quality of the underlying source probability model used by arithmetic coding. In particular, a more accurate estimate of  $\tilde{p}_{\text{LLM}}(t_{i+1} | \mathbf{t}_{1:i})$  yields a shorter compressed bitstream, which in turn reduces the vulnerability of the transmitted message to channel impairments.

To address these challenges, we propose the MASC scheme. As a transceiver-level paradigm, MASC integrates a Transformer-based backbone with a specialized PCM component to refine the source probability model. Within the PCM architecture, an MMER, denoted by  $\mathcal{R}(\cdot)$ , is employed to adaptively manage a set of multi-order  $n$ -gram memory modules:

$$\mathcal{M} = \left\{ \mathcal{M}^{(n)} \right\}_{n=2}^5, \quad (9)$$

where  $\mathcal{M}^{(n)}$  corresponds to the memory component associated

with the  $n$ -gram order<sup>2</sup>. To avoid activating all such components at every coding step, the MMER adaptively selects a sparse subset of relevant memory experts according to the current hidden state  $\mathbf{h}_i$ :

$$\mathcal{A}_i = \mathcal{R}(\mathbf{h}_i), \quad \mathcal{A}_i \subseteq \mathcal{M}, \quad (10)$$

where  $\mathcal{A}_i$  denotes the activated memory subset for the  $i$ -th token.

Under this architecture, the MASC-driven source encoding and decoding are formulated as  $\mathbf{m} = \mathcal{F}_{\text{MASC-AC}_s}(\mathbf{s}_{1:N_s})$  and  $\hat{\mathbf{s}} = \mathcal{F}_{\text{MASC-AC}_r}(\hat{\mathbf{m}})$ , respectively. Our objective is to jointly optimize the memory parameters within the PCM and the sparse routing strategy of the MMER to maximize reconstruction fidelity while adhering to a strict complexity budget. This is formulated as the following optimization problem:

$$\min_{\Theta} \mathbb{E}[d(\mathbf{s}_{1:N_s}, \hat{\mathbf{s}})] \quad \text{s.t.} \quad \text{Cost}(\mathcal{R}) \leq \mathcal{B}, \quad (11)$$

where  $\Theta$  denotes the learnable parameters of MASC,  $d(\cdot, \cdot)$  measures the reconstruction mismatch between the original source and the recovered sequence, and  $\mathcal{B}$  denotes the allowable routing complexity budget.

## III. MEMORY-AUGMENTED SOURCE CODING

As depicted in Fig. 2, the proposed MASC framework is built upon an Engram-style parameterized memory backbone, in which multi-order local contextual patterns are encoded

<sup>2</sup>Different from the original Engram backbone, which only uses the 2-gram and 3-gram memories, MASC extends the memory orders to 5 for better capturing long range contextual patterns.

through expert-specific hashed memories and injected into autoregressive source modeling via context-aware gated fusion. On top of this backbone, we further introduce an MMER to perform sparse, hidden-state-dependent expert selection, so that only the most relevant memory experts are activated at each coding step. Conditioned on the selected experts, the corresponding suffix  $n$ -gram contexts are used for expert-specific memory lookup, and the retrieved memories are subsequently fused back into the Transformer backbone.

#### A. Engram-Style Memory Backbone

We first describe the Engram-style hashed memory backbone [19], which serves as the basic memory lookup mechanism adopted in MASC. In this backbone, a Transformer models global autoregressive dependencies, while an external hashed memory module captures recurring local contextual patterns through multi-order  $n$ -gram memories. Specifically, as in Eq. (9), the memory backbone maintains order-specific hashed memories based on short local contexts. Given an input token sequence  $\mathbf{t}_{1:N_t} = (t_1, \dots, t_i, \dots, t_{N_t})$ , the suffix context of order  $n$  ending at position  $i \geq n$  is defined as

$$g_i^{(n)} = (t_{i-n+1}, \dots, t_i), \quad n \in \{2, \dots, 5\}. \quad (12)$$

Directly parameterizing all possible  $n$ -gram combinations is computationally prohibitive. Therefore, following the hashed-memory paradigm in Engram, each suffix context is mapped into a compact set of memory indices through deterministic hashing [25]. For the  $m \in 1, \dots, M$ -th hash head of the  $n$ -gram memory, we compute

$$z_i^{(n,m)} = \phi^{(n,m)}(g_i^{(n)}), \quad \mathbf{e}_i^{(n,m)} = \mathbf{E}^{(n,m)}[z_i^{(n,m)}], \quad (13)$$

where  $M$  is the number of hash heads,  $\phi^{(n,m)}(\cdot)$  is a hash function and  $\mathbf{E}^{(n,m)}$  denotes the corresponding embedding table. Accordingly, for the contexts ending at token  $i$ , the final memory representation  $\mathbf{e}_i$  is obtained by concatenating the hashed embeddings  $\mathbf{e}_i^{(n,m)}$ , which will be formally given later in Eq. (24).

After memory lookup, the retrieved memory representations are injected into the Transformer hidden states through a context-aware gating mechanism. Let  $\mathbf{h}_i^{(l)}$  denote the hidden state at token  $i$  in the  $l$ -th Transformer layer. The hidden state is used as the query, while the retrieved memory representation is projected into the key and value spaces [26]:

$$\mathbf{q}_i = \mathbf{h}_i^{(l)}, \quad \mathbf{k}_i = \mathbf{W}_K \mathbf{e}_i, \quad \mathbf{v}_i = \mathbf{W}_V \mathbf{e}_i, \quad (14)$$

where  $\mathbf{W}_K$  and  $\mathbf{W}_V$  are learnable projection matrices. The compatibility between the current hidden state and the retrieved memory is measured by

$$\beta_i = \sigma\left(\frac{\text{Norm}(\mathbf{q}_i)\text{Norm}(\mathbf{k}_i)}{\sqrt{d}}\right), \quad (15)$$

where  $\sigma(\cdot)$  denotes the sigmoid function,  $\text{Norm}(\cdot)$  denotes RMS normalization, and  $d$  is a scale constant. The gated memory output is then given by

$$\tilde{\mathbf{v}}_i = \beta_i \mathbf{v}_i. \quad (16)$$

Collecting the gated memory values of all tokens in the  $l$ -th Transformer layer, we obtain

$$\tilde{\mathbf{V}}^{(l)} = [\tilde{\mathbf{v}}_1, \tilde{\mathbf{v}}_2, \dots, \tilde{\mathbf{v}}_{N_t}]. \quad (17)$$

To further refine the gated memory sequence and introduce local nonlinear transformation, the Engram-style backbone applies a lightweight depthwise causal convolution:

$$\mathbf{Y}^{(l)} = \text{SiLU}\left(\text{Conv1D}\left(\text{Norm}\left(\tilde{\mathbf{V}}^{(l)}\right)\right)\right) + \tilde{\mathbf{V}}^{(l)}, \quad (18)$$

where  $\text{Conv1D}(\cdot)$  denotes a lightweight depthwise causal one-dimensional convolution, and  $\text{SiLU}(\cdot)$  denotes the Sigmoid Linear Unit activation function.

Finally, the refined memory output is injected into the Transformer backbone through a residual connection:

$$\mathbf{H}^{(l)} \leftarrow \mathbf{H}^{(l)} + \mathbf{Y}^{(l)}. \quad (19)$$

#### B. MMER-Based Sparse Expert Routing

Although the Engram-style backbone provides multi-order memory representations, the most informative contextual granularity is usually token-dependent. For example, some next-token predictions are mainly determined by short-range collocations, whereas others require longer local contexts. Therefore, instead of activating all memory experts at each coding step, MASC introduces an MMER to perform sparse and hidden-state-dependent expert selection.

Given the hidden state  $\mathbf{h}_i^{(l)}$  in the  $l$ -th Transformer layer, MMER computes routing logits over the four experts associated with  $n$ -gram memories as

$$\mathbf{r}_i = \mathbf{W}_r \text{Norm}\left(\mathbf{h}_i^{(l)}\right) \in \mathbb{R}^4, \quad (20)$$

where  $\mathbf{W}_r$  is a learnable projection matrix. The routing probabilities are then obtained by

$$\boldsymbol{\pi}_i = \text{softmax}(\mathbf{r}_i). \quad (21)$$

To enforce sparse activation, only the top- $k$  experts are retained:

$$\mathcal{A}_i = \text{TopK}(\boldsymbol{\pi}_i, k) \subseteq \{2, 3, 4, 5\}, \quad |\mathcal{A}_i| = k. \quad (22)$$

Let  $\{\alpha_i^{(n)}\}_{n \in \mathcal{A}_i}$  denote the normalized routing weights over the selected experts, given by

$$\alpha_i^{(n)} = \frac{\pi_i^{(n)}}{\sum_{j \in \mathcal{A}_i} \pi_i^{(j)}}, \quad n \in \mathcal{A}_i, \quad (23)$$

where  $\pi_i^{(n)}$  denotes the routing probability assigned to the  $n$ -gram expert.

In this way, MMER adaptively identifies the most relevant contextual granularities while avoiding the unnecessary activation of irrelevant memory experts at every step.

### C. MMER-Conditioned Memory Retrieval

Different from the original Engram backbone, which fixedly aggregates the 2-gram and 3-gram memories, MASC performs routing-weighted aggregation over the selected experts:

$$\mathbf{e}_i = \sum_{n \in \mathcal{A}_i} \alpha_i^{(n)} \mathbf{e}_i^{(n)}. \quad (24)$$

Here, the memory representation  $\mathbf{e}_i^{(n)}$ , corresponding to  $n$ -gram hashed memory for the context ending at token  $i$ , can be written as  $\mathbf{e}_i^{(n)} = \parallel_{m=1}^M \mathbf{e}_i^{(n,m)}$ ,  $n \in \mathcal{A}_i$ , where  $\parallel$  denotes the concatenation operation,  $\alpha_i^{(n)}$  is the normalized routing weight assigned by MMER, as defined in (23). The resulting  $\mathbf{e}_i$  is then injected into the backbone described in Section III-A.

### D. Training Objective

The proposed MASC is optimized with a next-token prediction objective, while an auxiliary routing loss is introduced to regularize expert utilization. Given an input token sequence  $\mathbf{t}_{1:N_t}$ , the model predicts the next token at each position and is optimized by the standard Cross-Entropy (CE) loss

$$\mathcal{L}_{\text{CE}} = -\frac{1}{|\Omega|} \sum_{i \in \Omega} \log \tilde{p}_{\text{MASC}}(t_{i+1} \mid \mathbf{t}_{1:i}), \quad (25)$$

where  $\Omega$  denotes the set of valid prediction positions excluding padded tokens, and  $\tilde{p}_{\text{MASC}}(\cdot)$  denotes the next-token distribution produced by the MASC source model.

To avoid degenerate routing behavior in MMER, we further introduce an auxiliary load-balancing loss to encourage a more even utilization of the memory experts. Let  $\pi_i$  denote the soft routing probability for  $i$ -th token, and  $\mathcal{A}_i$  denote the corresponding hard-selected top- $k$  expert subset. We first define the expert importance as the average soft routing mass:

$$\text{Imp}_n = \frac{1}{N_t} \sum_{i=1}^{N_t} \pi_i^{(n)}, \quad n \in \{2, 3, 4, 5\}, \quad (26)$$

and the expert load as the average hard selection frequency:

$$\text{Load}_n = \frac{1}{kN_t} \sum_{i=1}^{N_t} \mathbb{I}(n \in \mathcal{A}_i), \quad n \in \{2, 3, 4, 5\}, \quad (27)$$

where  $\mathbb{I}(\cdot)$  is the indicator function. Based on these quantities, the auxiliary routing loss is defined as

$$\mathcal{L}_{\text{aux}} = 4 \sum_{n \in \{2, 3, 4, 5\}} \text{Imp}_n \text{Load}_n. \quad (28)$$

The overall training objective is then given by

$$\mathcal{L} = \mathcal{L}_{\text{CE}} + \lambda_{\text{aux}} \mathcal{L}_{\text{aux}}, \quad (29)$$

where  $\lambda_{\text{aux}}$  is a balancing coefficient.

## IV. SIMULATION SETTINGS AND RESULTS

### A. Simulation Settings

We evaluate the proposed MASC scheme against conventional SSCC pipelines and representative JSCC-based semantic communication schemes over both Rayleigh and AWGN fading channels. To ensure a fair and reproducible comparison, all methods are tested on the same text source and are assessed using widely adopted Natural Language Processing (NLP)-oriented quality metrics [27], [28].

**Dataset and source coding.** The adopted dataset is the English portion of the Europarl corpus [29]. We preprocess the raw text by removing XML tags and speaker identifiers, splitting long lines into sentence-level samples at punctuation marks, and removing duplicate sentences. The resulting samples are then randomly shuffled with a fixed seed and partitioned into training, validation, and test sets with a ratio of 80%/10%/10%. For the conventional SSCC baselines, including LLM-AC with ECCT and LLM-AC with ECCT and ICD, we adopt a standard GPT-2-based [30] source model. In contrast, Engram-AC with ECCT and the proposed MASC employ their own trained memory-augmented source models, with the latter further integrating a PCM equipped with an MMER. The arithmetic coder is configured with a precision of 31 bits, which provides a practical trade-off between numerical stability and coding accuracy.

**Channel coding and ECCT configuration.** For the SSCC-based pipelines, we employ an LDPC(49, 24) code, corresponding to a code rate of approximately 0.5. On the receiver side, ECCT is adopted as a complementary channel decoding module to improve codeword recovery under severe noise.

**Baselines.** We include the following representative baselines:

- **Engram-AC with ECCT** [19], which combines ECCT-assisted channel decoding with an Engram-enhanced source model for arithmetic source coding/decoding under the SSCC pipeline.
- **LLM-AC with ECCT and ICD** [18], which augments the ECCT-assisted LLM-based SSCC pipeline with receiver-side contextual information and candidate-based reconstruction.
- **LLM-AC with ECCT** [7], which combines ECCT-assisted channel decoding with LLM-based lossless source coding/decoding under the SSCC pipeline.
- **Huffman with ECCT**, where the LLM-driven arithmetic source coding/decoding is replaced by Huffman coding, while keeping the rest of the SSCC pipeline unchanged.
- **DeepSC** [20] and **UT** [21], which serve as representative JSCC baselines for comparison.
- **UT with quantization** [22], where the continuous latent representation is mapped to a fixed-length bitstream (30 bits) for transmission.

**Evaluation metrics.** We evaluate reconstruction quality using Bilingual Evaluation Understudy (BLEU) [27] and a Bidirectional Encoder Representations from Transformers (BERT)-based semantic similarity metric [28], which measure

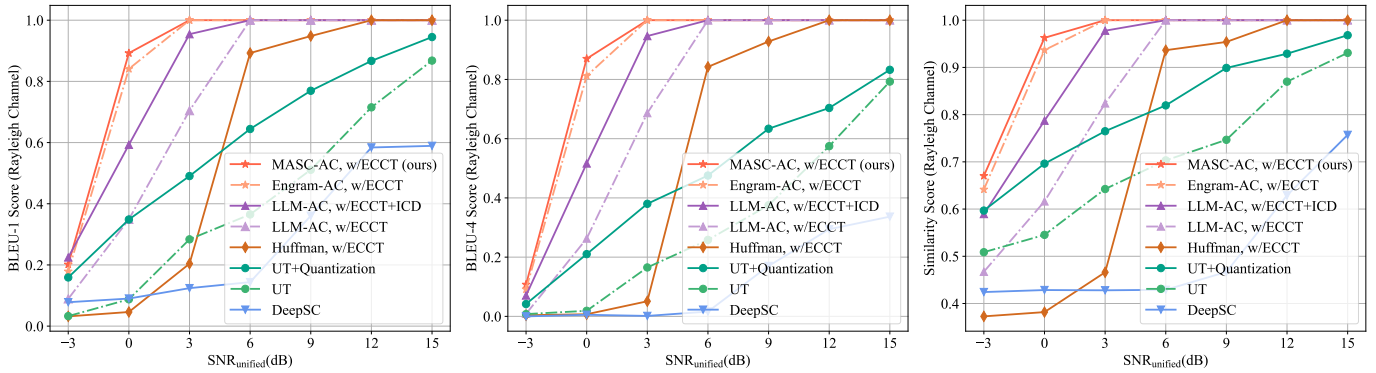


Fig. 3. Overall system-level performance under Rayleigh channels.

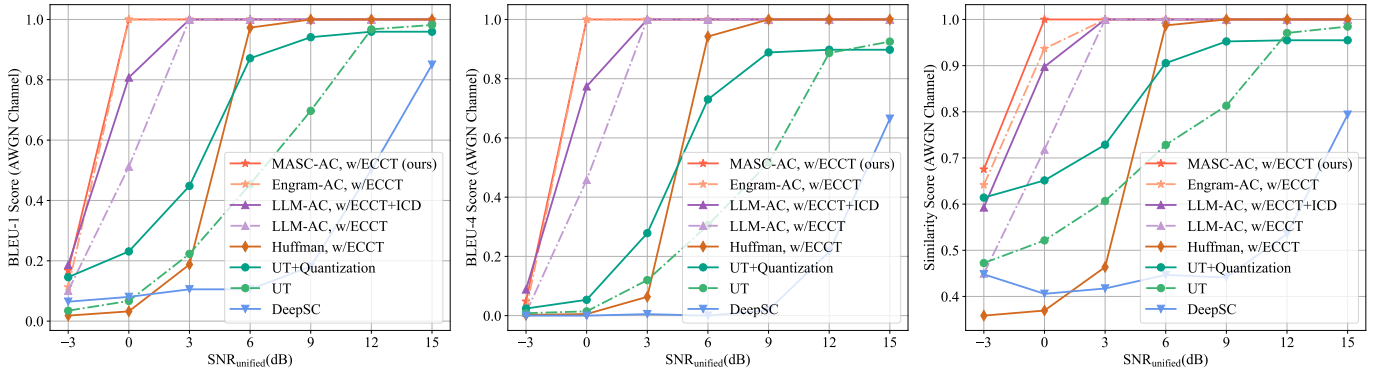


Fig. 4. Overall system-level performance under AWGN channels.

lexical fidelity and semantic preservation, respectively. To fairly compare heterogeneous pipelines that may transmit different physical-layer payload lengths  $N$  for the same source content, we follow [7] and adopt a unified SNR under a fixed total transmission energy budget.

### B. Overall System-Level Performance Comparison

Fig. 3 and Fig. 4 present the system-level overall performance comparison between the proposed method and multiple baselines over Rayleigh and AWGN channels, respectively, evaluated by BLEU-1, BLEU-4, and semantic similarity.<sup>3</sup> It is observed that MASC consistently outperforms the conventional SSCC baselines, including Huffman with ECCT and LLM-AC with ECCT, as well as the representative JSCC schemes under both channel models. MASC also achieves uniformly better performance than the Engram-based scheme, confirming the effectiveness of introducing MMER-based sparse expert selection on top of the shared memory-augmented source modeling framework. The gain is particularly pronounced in the low-SNR regime, where improved conditional probability modeling yields shorter codewords and thus mitigates the susceptibility of arithmetic decoding to residual channel errors. Furthermore, MASC generally exhibits better performance than ICD. It is worth emphasizing that ICD

operates under a stronger assumption of perfectly reliable contextual information at the receiver, whereas MASC achieves robustness enhancement through transceiver-level memory-augmented source modeling in a self-contained manner.

## V. CONCLUSIONS

In this work, we have presented MASC, a memory-augmented source coding scheme for robust SSCC-based transmission in low-SNR regimes. Motivated by the cliff effect caused by the catastrophic propagation of residual channel errors through autoregressive source decoding, MASC has internalized recurring contextual patterns into a shared source model used consistently by both the transmitter and the receiver. Specifically, the proposed PCM has captured multi-order  $n$ -gram patterns for source probability modeling, while the MMER has enabled sparse, hidden-state-dependent routing over memory experts for adaptive and efficient memory utilization during autoregressive source coding. Extensive evaluations over Rayleigh and AWGN fading channels have demonstrated the effectiveness of the proposed scheme relative to conventional SSCC baselines, representative JSCC schemes, and receiver-side in-context decoding methods. In future work, we will extend the current memory design toward richer memory representations and more adaptive routing mechanisms for broader multimodal transmission scenarios.

<sup>3</sup>Additional experiments are in progress and will be included in an extended version.

## REFERENCES

- [1] K. Lu, *et al.*, “Rethinking modern communication from semantic coding to semantic communication,” *IEEE Wireless Commun.*, vol. 30, no. 1, pp. 158–164, May 2023.
- [2] Y. Shao, *et al.*, “A theory of semantic communication,” *IEEE Trans. Mob. Comput.*, vol. 23, no. 12, pp. 12 211–12 228, Dec. 2024.
- [3] Z. Lu, *et al.*, “Semantics-empowered communications: A tutorial-cum-survey,” *IEEE Commun. Surv. Tutorials*, vol. 26, no. 1, pp. 41–79, Mar. 2024.
- [4] W. Zhang, *et al.*, “DeepMA: End-to-end deep multiple access for wireless image transmission in semantic communication,” *IEEE Trans. Cognit. Commun. Networking*, vol. 10, no. 2, pp. 387–402, Apr. 2024.
- [5] J. Huang, *et al.*, “D<sup>2</sup>-JSCC: Digital deep joint source-channel coding for semantic communications,” *IEEE J. Sel. Areas Commun.*, vol. 43, no. 4, pp. 1246–1261, Apr. 2025.
- [6] S. Tong, *et al.*, “Alternate learning-based snr-adaptive sparse semantic visual transmission,” *IEEE Trans. Wireless Commun.*, vol. 24, no. 2, pp. 1737–1752, Feb. 2025.
- [7] T. Ren, *et al.*, “Separate source channel coding is still what you need: An LLM-based rethinking,” *arXiv preprint arXiv:2501.04285*, 2025.
- [8] J. Huang, *et al.*, “Deep separate source-channel coding for semantic-aware image communications,” in *Proc. IEEE Int. Conf. Commun., ICC*, Rome, Italy, May 2023.
- [9] J. Huang, *et al.*, “Joint task and data-oriented semantic communications: A deep separate source-channel coding scheme,” *IEEE Internet Things J.*, vol. 11, no. 2, pp. 2255–2272, Jan. 2024.
- [10] Y. Choukroun, *et al.*, “Error correction code transformer,” in *Proc. Adv. Neural Inf. Proces. Syst., NIPS*, New Orleans, LA, USA, Nov. 2022.
- [11] S.-J. Park, *et al.*, “Multiple-masks error correction code transformer for short block codes,” *IEEE J. Sel. Areas Commun.*, vol. 43, no. 7, pp. 2518–2529, Jul. 2025.
- [12] H. Xie, *et al.*, “Semantic communication with memory,” *IEEE J. Sel. Areas Commun.*, vol. 41, no. 8, pp. 2658–2669, Jun. 2023.
- [13] D. Gündüz, *et al.*, “Beyond transmitting bits: Context, semantics, and task-oriented communications,” *IEEE J. Sel. Areas Commun.*, vol. 41, no. 1, pp. 5–41, Nov. 2023.
- [14] Y. Liu, *et al.*, “Extended context-based semantic communication system for text transmission,” *Digital Commun. Networks*, vol. 10, no. 3, pp. 568–576, Jun. 2024.
- [15] Y. Ren, *et al.*, “A sequence repetition node-based successive cancellation list decoder for 5G polar codes: Algorithm and implementation,” *arXiv preprint arXiv:2205.08857*, 2022.
- [16] I. Sagitov, *et al.*, “Generalized restart mechanism for successive-cancellation flip decoding of polar codes,” *J. Signal Process. Syst.*, vol. 97, no. 1, pp. 11–29, Apr. 2025.
- [17] C. Meister, *et al.*, “Locally typical sampling,” *arXiv preprint arXiv:2202.00666*, 2022.
- [18] Z. Wang, *et al.*, “In-context source and channel coding,” *arXiv preprint arXiv:2601.10267*, 2026.
- [19] X. Cheng, *et al.*, “Conditional memory via scalable lookup: A new axis of sparsity for large language models,” *arXiv preprint arXiv:2601.07372*, 2026.
- [20] H. Xie, *et al.*, “Deep learning enabled semantic communication systems,” *arXiv preprint arXiv:2006.10685*, 2020.
- [21] Q. Zhou, *et al.*, “Semantic communication with adaptive universal transformer,” *IEEE Wireless Commun. Lett.*, vol. 11, no. 3, pp. 453–457, Mar. 2022.
- [22] Q. Zhou, *et al.*, “Adaptive bit rate control in semantic communication with incremental knowledge-based HARQ,” *arXiv preprint arXiv:2203.06634*, 2022.
- [23] I. H. Witten, *et al.*, “Arithmetic coding for data compression,” *Commun. ACM*, vol. 30, no. 6, p. 520–540, Jun. 1987.
- [24] E. Arikan, “Channel polarization: A method for constructing capacity-achieving codes for symmetric binary-input memoryless channels,” *IEEE Trans. Inf. Theory*, vol. 55, no. 7, pp. 3051–3073, Jul. 2009.
- [25] D. Tito Svenstrup, *et al.*, “Hash embeddings for efficient word representations,” in *Proc. Adv. Neural Inf. Proces. Syst., NIPS*, Dec. 2017.
- [26] A. Vaswani, “Attention is all you need,” in *Proc. Adv. Neural Inf. Proces. Syst., NIPS*, Long Beach, CA, USA, Dec. 2017.
- [27] K. Papineni, *et al.*, “BLEU: a method for automatic evaluation of machine translation,” in *Proc. ACL*, Philadelphia, Pennsylvania, USA, Jul. 2002.
- [28] J. Devlin, *et al.*, “BERT: Pre-training of deep bidirectional transformers for language understanding,” in *Proc. Conf. N. Am. Chapter Assoc. Comput. Linguistics: Hum. Lang. Technol.*, Minneapolis, Minnesota, Jun. 2019.
- [29] P. Koehn, “Europarl: A parallel corpus for statistical machine translation,” in *Proc. MTSummit*, Phuket, Thailand, Sep. 2005.
- [30] A. Radford, *et al.*, “Language models are unsupervised multitask learners,” OpenAI Technical Report, 2019, [Online]. Available: [https://cdn.openai.com/better-language-models/language\\_models\\_are\\_unsupervised\\_multitask\\_learners.pdf](https://cdn.openai.com/better-language-models/language_models_are_unsupervised_multitask_learners.pdf). [Online]. Available: [https://cdn.openai.com/better-language-models/language\\_models\\_are\\_unsupervised\\_multitask\\_learners.pdf](https://cdn.openai.com/better-language-models/language_models_are_unsupervised_multitask_learners.pdf)